Analysis and Design of Full-Band Matched Waveguide Bends

Mauro Mongiardo, Antonio Morini, and Tullio Rozzi, *Fellow, IEEE*

Abstract— **Compact waveguide bends with low return loss over the full waveguide band width are realized by placing properly selected discontinuities inside the curve. The component is designed by using an extremely efficient computer code which employs the *local modes* approach to analyze curved sections, while discontinuities are rigorously accounted for by considering their multimode equivalent circuit. A simple technique to select the appropriate matching elements is described and examples of full-band matched bends are provided.**

I. Introduction

WAVEGUIDE BENDS are crucial for sophisticated microwave systems such as radar seekers, satellite beam forming networks, etc., [1]–[3], where, in order to minimize space requirements, it is often required to realize compact bends, i.e., curves with short radii, but nevertheless exhibiting low return loss over a wide band. Wide-band matched (WBM) bends were first introduced by de Ronde [4] by inserting suitable matching elements (ME) such as stubs, notches, etc., mainly on an experimental basis.

While a considerable amount of literature addresses the full-wave analysis of bends [5]–[11], apart for a few cases [12], [13] there is a lack of information on the design of compact WBM bends. Moreover, most current approaches do not coexist favorably with the commonest method used for analyzing interacting discontinuities. This method, in fact, is based on the use of the generalized scattering matrices (GSM), considering all the accessible modes relative to each discontinuity. It would be appropriate, therefore, to characterize the bend too in terms of its GSM. As an example, numerically oriented methods, although useful for analysis purposes, fail to provide insight on how to select suitable ME, while their limited numerical efficiency prevents their use in the optimization routines necessary to design WBM components.

In this contribution we present a method to design compact *full-band matched* (FBM) bends, which are easy to manufacture, avoiding the use of trimming elements and providing a fairly robust design from both the electrical and mechanical viewpoints. The proposed matching method is based on the analysis of bends under even and odd excitation. It is noted that, by introducing a thin metal iris in the symmetry plane of the bend, only the even susceptance is changed. By taking advantage of the bend frequency response, it is possible to properly adjust the metal iris in such a way as to alter the even susceptance and to achieve full band matching.

In addition, we also introduce the combination of the local modes concept [14] and that of accessible modes, that is particularly well suited to account for the presence of discontinuities and ME's inside the bend. Thanks to its numerical efficiency, this approach is an ideal candidate for CAD purposes.

The next two sections illustrate the local modes analysis of H-plane and E-plane bends, respectively. In both cases it is seen that the presence of the bend causes modal coupling which is *rigorously* described by a system of generalized telegrapher's equations. The solution of the latter system is described in Section IV, while Section V describes some results for the unmatched bend. The last section, Section VI, illustrates the technique for FBM bends and provides some examples.

II. Analysis of H-Plane Bends by Local Modes

Let us consider a rectangular waveguide H-plane bend of angle θ, as shown in schematic top view in Fig. 1, under fundamental TE_{10} mode incidence. This mode has no variation in the y-direction and its only field components are E_y, H_x, H_z. The method of local modes describes the field in each section of the bend by means of a *superposition of modes of the locally straight waveguide*. In this way, the electric field in the bend is expressed as a superposition of the modes $\phi_n(x) = \sqrt{\frac{2}{a}} \sin \frac{n\pi x}{a}$ in the following manner

$$E_y(x,z) = \sum_{n=1}^{\infty} V_n(z)\phi_n(x) \tag{1}$$

while the magnetic field is given by

$$H_x(x,z) = -\sum_{n=1}^{\infty} I_n(z)\phi_n(x). \tag{2}$$

In practice, sums are truncated after few terms, say N, since the bend is a smooth discontinuity. While modes in a straight section are independent of each other, in curved sections they couple and their propagation is described by the following system of equations

$$\partial_\varphi V_m = -A_m I_m - \sum_{n=1}^{N} B_{mn} I_n \tag{3}$$

$$\partial_\varphi I_m = -C_m V_m - \sum_{n=1}^{N} D_{mn} V_n \tag{4}$$

Manuscript received March 7, 1995; revised July 10, 1995. This work was supported in part by MURST.

M. Mongiardo is with the Istituto di Elettronica, Università di Perugia, I-06100 Perugia, Italy.

A. Morini and T. Rozzi are with the Dipartimento di Elettronica ed Automatica, Università di Ancona, 60131, Ancona, Italy.

IEEE Log Number 9415456.

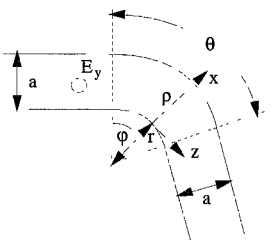

Fig. 1. H-plane bend showing coordinate systems used.

where the coefficients A_m, B_m, C_{mn}, D_{mn}, have the simple close-form expressions derived below.

A. Coefficients of the Telegrapher's Equation

In each section of the bend the field may be obtained from a potential ψ solution of the Helmholtz' equation expressed in cylindrical coordinates, i.e.,

$$\left(\partial_\rho^2 + \frac{1}{\rho}\partial_\rho\right)\psi + \frac{1}{\rho^2}\partial_\varphi^2\psi + k^2\psi = 0. \tag{5}$$

From which the transverse field components are obtained in cylindrical coordinates, as

$$\begin{aligned} E_y &= j\omega\mu\psi \\ H_\rho &= \frac{1}{\rho}\partial_\varphi\psi. \end{aligned} \tag{6}$$

In order to find the actual form of the field we make use of the expansion (1) and (2). Note that in these expansions the $\phi_n(x)$ constitute a complete, orthonormal, basis, but they are *not* the modal basis for our curved section. In fact, the $\phi_n(x)$ are the modal function of the *straight* waveguide; as such they satisfy the following wave equation

$$\partial_x^2\phi_n + k^2\phi_n = \beta_n^2\phi_n \tag{7}$$

where β_n is the propagation constant.

With reference to Fig. 1, the relationship between the cylindrical and the rectangular coordinate system is provided by

$$\begin{aligned} \partial_z &= \frac{1}{\rho}\partial_\varphi \\ \rho &= r + x \\ \partial_x &= \partial_\rho. \end{aligned} \tag{8}$$

By substituting the expansion (1) and (2) into (6) and (5) it is possible to obtain the two generalized telegrapher's equation linking voltages and currents along the bend as described in the following.

First Generalized Telegrapher's Equation: By substituting (1) and (2) into (6), noting that $H_x = H_\rho$, yields

$$\sum_{n=1}^{N}\partial_\varphi V_n\phi_n = -j\omega\mu\rho\sum_{n=1}^{N} I_n\phi_n. \tag{9}$$

By taking advantage of the orthonormality of the basis functions ϕ_n, (9) provides the first of the generalized telegrapher's equations, i.e.,

$$\partial_\varphi V_m = -j\omega\mu r I_m - j\omega\mu\sum_{n=1}^{N} H_{mn}I_n \tag{10}$$

where we have introduced the following coupling terms

$$H_{mn} = \langle\phi_m, x\phi_n\rangle. \tag{11}$$

Equation (10) clearly shows that mode coupling takes place in the bend. In particular, for H-plane bends the coupling terms H_{mn} are given by

$$\begin{aligned} H_{mn} &= \frac{2}{a}\int_0^a x\sin\left(\frac{m\pi}{a}x\right)\sin\left(\frac{n\pi}{a}x\right)dx \\ &= \begin{cases} \frac{a}{2} - \frac{a}{\pi^2(m+n)^2}[\cos(m+n)\pi - 1] & m = n \\ \frac{a}{\pi^2(m-n)^2}[\cos(m-n)\pi - 1] & \\ -\frac{a}{\pi^2(m+n)^2}[\cos(m+n)\pi - 1] & m \neq n \end{cases}. \end{aligned} \tag{12}$$

Second Generalized Telegrapher's Equation: In order to derive the second generalized telegrapher's equation it is expedient to note that, by using (8) the first term in (5) may be written as

$$\left(\partial_\rho^2 + \frac{1}{\rho}\partial_\rho\right)\psi = \partial_x^2\psi + \frac{1}{(r+x)}\partial_x\psi \tag{13}$$

while, by using (6), the second term in (5) yields

$$\frac{1}{\rho^2}\partial_\varphi^2\psi = \frac{1}{\rho}\partial_\varphi H_\rho = -\frac{1}{\rho}\sum_{n=1}^{N}\partial_\varphi I_n(\varphi)\phi_n(x). \tag{14}$$

After inserting the two above equations into (5) and by using (7), we get

$$\sum_{n=1}^{N}(r+x)\beta_n^2 V_n\phi_n + \sum_{n=1}^{N} V_n\frac{\partial\phi_n}{\partial x} = j\omega\mu\sum_{n=1}^{N}\frac{\partial I_n}{\partial\varphi}\phi_n. \tag{15}$$

Taking advantage of mode orthonormality, one finally obtains

$$\frac{\partial I_m}{\partial\varphi} = -j\frac{\beta_m^2 r}{\omega\mu}V_m - j\sum_{n=1}^{N}\left(\frac{\beta_n^2}{\omega\mu}H_{mn} + \frac{f_{mn}}{\omega\mu}\right)V_n \tag{16}$$

where the following coupling integral is introduced

$$\begin{aligned} f_{mn} &= \left\langle\phi_m, \frac{\partial\phi_n}{\partial x}\right\rangle = \frac{2}{a}\frac{n\pi}{a}\int_0^a \sin\left(\frac{m\pi}{a}x\right)\cos\left(\frac{n\pi}{a}x\right)dx \\ &= \begin{cases} 0 & m = n \\ \frac{n}{a}\left\{\frac{[1-(-1)^{m+n}](m-n)+[1-(-1)^{m-n}](m+n)}{m^2-n^2}\right\} & m \neq n \end{cases}. \end{aligned} \tag{17}$$

By rewriting (10) and (16) and using for brevity the quantities

$$\begin{aligned} A_m &= j\omega\mu r \quad B_{mn} = j\omega\mu H_{mn} \\ C_m &= j\frac{\beta_m^2 r}{\omega\mu} \quad D_{mn} = j\left(\frac{\beta_n^2}{\omega\mu}H_{mn} + \frac{f_{mn}}{\omega\mu}\right) \end{aligned} \tag{18}$$

we get the system of (3) and (4). This gives the differential relationships between voltages and currents expressing the amplitude of the electric and magnetic fields, respectively, along the bend. The solution of the telegrapher's (3), (4) is obtained as described in Section IV.

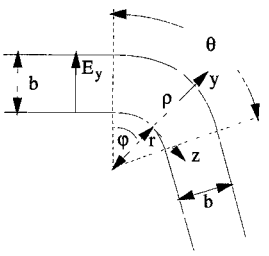

Fig. 2. E-plane bend showing coordinate systems used.

III. Analysis of E-Plane Bends by Local Modes

For the analysis of E-plane bends it is expedient to derive the field from an LSE Hertzian potential $\hat{x}\psi_h$ which, in each section of the bend, is represented by a summation of local modes, each satisfying "local" boundary conditions. Referring to the two coordinate systems shown in Fig. 2, the global one (ρ, φ, x), and the local one (y, z, x), we express the Hertzian potential as

$$\psi_h(x,y,z) = \sum_{n=0,1}^{\infty} a_n(z)\psi_n(y)\varphi(x) \tag{19}$$

where

$$\varphi(x) = \sqrt{\frac{2}{a}} \sin \frac{\pi}{a} x \tag{20}$$

expresses the x-dependence that is always the same along the bend, while

$$\psi_n(y) = \frac{\epsilon_n}{\sqrt{b}} \cos \frac{n\pi}{b} y \quad \epsilon_0 = 1, \quad \epsilon_n = \sqrt{2}. \tag{21}$$

The coefficients $a_n(z(\varphi))$ must be chosen in such a way that the potential ψ_h satisfies the wave equation, expressed in the cylindrical coordinate system associated to the bend

$$\left(\partial_\rho^2 + \frac{1}{\rho}\partial_\rho + \frac{1}{\rho^2}\partial_\varphi^2 + \beta_{10}^2\right)\psi_h = 0. \tag{22}$$

Now, from the property of the expansion to be local it follows that

$$\partial_z \psi_h = \frac{1}{\rho}\partial_\phi \psi_h = \sum_{n=0,1}^{\infty} b_n(z)\psi_n(y)\varphi(x). \tag{23}$$

By noting that

$$\rho = r + y \quad \partial_\rho = \partial_y \quad \frac{1}{\rho}\partial_\varphi = \partial_z \tag{24}$$

we obtain the following system of coupled equations in the unknown coefficients $a_n(\varphi)$, $b_n(\varphi)$

$$\begin{aligned}
\partial_\varphi a_m &= \sum_{n=0,1}^{\infty} \langle (r+y)\psi_m, \psi_n\rangle b_n \\
\partial_\varphi b_m &= \sum_{n=0,1}^{\infty} \Gamma_n^2 \langle (r+y)\psi_m, \psi_n\rangle a_n \\
&\quad - \sum_{n=0,1}^{\infty} \langle \psi_m, \psi_n'\rangle a_n.
\end{aligned} \tag{25}$$

Where prime denotes derivative and Γ_n denotes the propagation constant of the LSE_{1n} mode. In the above equation the inner product is defined as $\langle f, g\rangle = \int_0^b fg\,dy$. By using standard definitions, the previous equations are cast in terms of normalized modal voltages and currents i_n, v_n as

$$\begin{aligned}
\partial_\varphi v_m &= \Gamma_m r i_m + \sum_{n=0,1}^{\infty} \frac{\Gamma_n^2}{\sqrt{\Gamma_m \Gamma_n}} \langle y\psi_m, \psi_n\rangle i_n \\
&\quad - \sum_{n=0,1}^{\infty} \frac{1}{\sqrt{\Gamma_m \Gamma_n}} \langle \psi_m, \psi_n'\rangle i_n \\
\partial_\varphi i_m &= \Gamma_m r v_m + \sum_{n=0,1}^{\infty} \sqrt{\Gamma_m \Gamma_n} \langle y\psi_m, \psi_n\rangle v_n.
\end{aligned} \tag{26}$$

These are again in the form of generalized telegrapher's equations.

IV. Solution of the Telegrapher's Equations

By introducing an appropriate matrix $[\tau]$ the generalized telegrapher's equations (3), (4) for the H-plane bend and (26) for the E-plane bend, respectively, are rewritten in the following way

$$\partial_\varphi \begin{bmatrix} \mathbf{v} \\ \mathbf{i} \end{bmatrix} = [\tau] \begin{bmatrix} \mathbf{v} \\ \mathbf{i} \end{bmatrix}. \tag{27}$$

For a bend of angle θ and constant radius the matrix $[\tau]$ is a constant, thus allowing solution of the above system in the form

$$\begin{bmatrix} \mathbf{v} \\ \mathbf{i} \end{bmatrix} = e^{\theta[\tau]} \begin{bmatrix} \mathbf{v} \\ \mathbf{i} \end{bmatrix}_0 \tag{28}$$

where the subscript 0 in the r.h.s. term stands for the voltage and current distribution at $\phi = 0$. The matrix $e^{\theta[\tau]}$, i.e., the ABCD transmission matrix of the bend, is computed by using the formula

$$\begin{bmatrix} \mathbf{A} & \mathbf{B} \\ \mathbf{C} & \mathbf{D} \end{bmatrix} = e^{\theta[\tau]} = \sum_{n=0,1}^{\infty} \frac{(\theta[\tau])^n}{n!}. \tag{29}$$

In order to overcome any numerical instability arising from the use of the transmission matrix with several modes below cut-off, it is expedient to compute the solution for a small angle $\Delta\varphi = \frac{\theta}{2^M}$ and then to transform the transmission matrix into the scattering matrix. Calling $S_{\Delta\varphi}$ the latter , the generalized scattering matrix of the entire bend, S_θ is given by the formula

$$S_\theta = F^M(S_{\Delta\varphi}). \tag{30}$$

Where the operator F computes the scattering matrix resulting from cascading two identical junctions. This approach, apart for being numerically efficient and very stable, is also well suited to deal with matching elements inside the bend. In fact, it is easy to analyze the effects of a discontinuity by describing the latter in terms of its accessible modes. Note that, by numerically solving (27), the local mode technique also allows to consider bends with varying angle of curvature, as well as serpentines, etc.

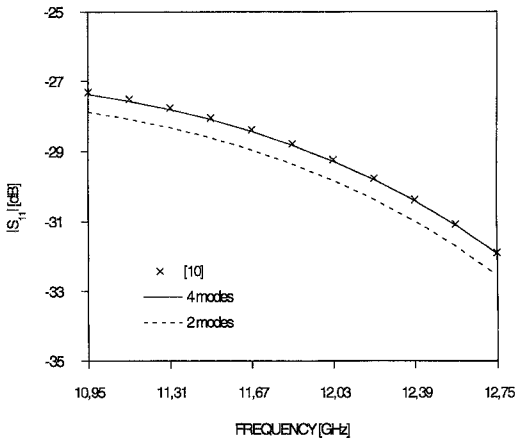

Fig. 3. Reflection coefficient of an E-plane 90° bend of radii $R = r+b/2 = 10$ mm in WR75. Crosses refer to the experimental results of [10].

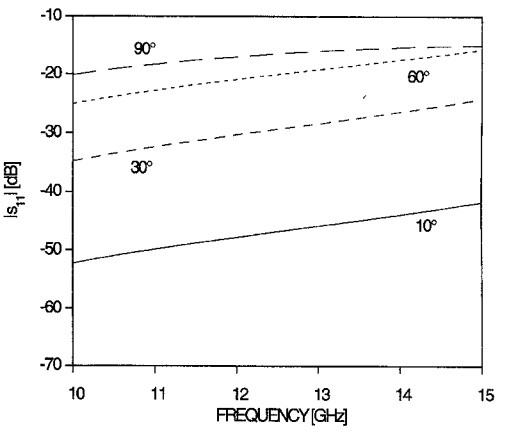

Fig. 4. Reflection coefficient of E-plane bends of radius $R = r + b/2 = 6$ mm in WR75 for different angles.

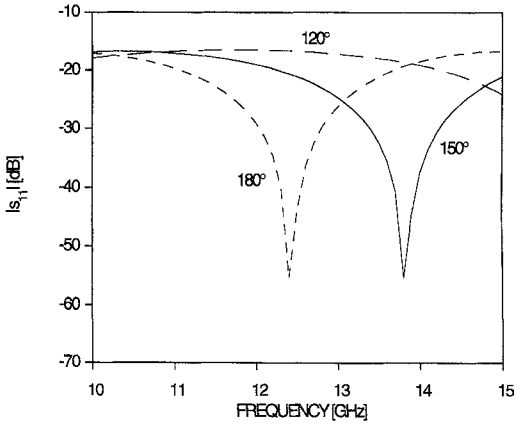

Fig. 5. Reflection coefficient of E-plane bends of radius $R = r + b/2 = d$ 6 mm in WR75 for different angles.

V. Results for Unmatched Bends

FORTRAN computer codes, based on the local modes approach, have been developed and tested against published data for unmatched bends both in the E- and H-planes. For the latter, several comparisons with experimental data and other numerical solutions have been already reported in the digest version and are not considered here, where we concentrate on E-plane bends.

A. Convergence Analysis

In Fig. 3 our numerical results are compared with those measured by [10]. It is apparent that a very good agreement is present. It is also noted that fairly good results are obtained by considering the coupling of just *two* modes. In fact, when using four modes only modest differences are noticed. Also, we checked the method by further increasing the number of modes, finding responses indistinguishable from those obtained considering 4 modes.

Since similar conclusions also hold for the H-plane case, it seems fair to say that, in order to obtain very accurate results, less than 4 modes need be considered. Moreover, fairly accurate results are obtained by considering just two modes, provided that one or more resonances do not occur over the band. In that case, the first two modes cancel each other and the role played by the higher order modes can become significant; This occurs, for instance, for the 180° bend shown in the following: the model employing two local modes can only supply a semiquantitative idea of the response, but an accurate determination of the resonance requires at least 4 local modes.

B. Effect of the Bend Angle

The effects of the bend angle on the reflection coefficients have been investigated as shown in Figs. 4 and 5. It is apparent that, even for the small radius of curvature considered, very small reflections arise when the bend angle is less than 30°. For larger angles the reflected power increases, thus making necessary the presence of matching elements in order to compensate such reflections. Similarly to the H-plane case, it is noted that, for a particular combination of radius and bend angle, we may have a very low reflection coefficient. As an example the latter occurs in Fig. 5, for a radius of 6 mm and a bend angle of 180° at the frequency of 12.4 GHz. The knowledge of this angle is of some relevance since it may allow the design of rather complicated network without return losses due to bends. However, it is clear that the bend is matched only over a modest bandwidth. In order to obtain *full-band matched* bends, it is necessary to properly insert matching elements as described in the next section.

VI. Full Band Matched E-Plane Bends

The study of the 90° bend under even and odd excitation, with respect to the symmetry plane, provides considerable insight into the problem of matching. In fact, it is found that the normalized input reactances X_e and X_o, for the even (magnetic wall in the symmetry plane) and the odd case (electric wall in the symmetry plane), respectively, are approximately related to each other, over the entire band, via the following formula

$$X_e = -\left(\frac{1}{X_o} + \chi\right). \tag{31}$$

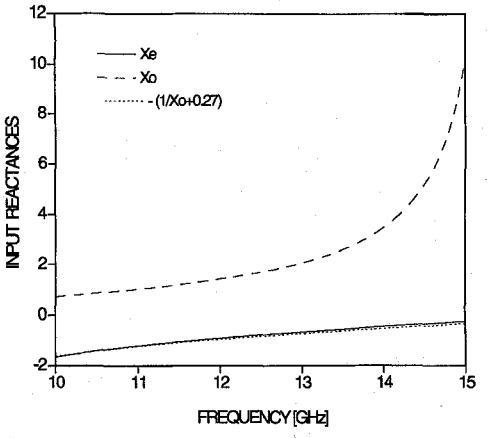

Fig. 6. Even and odd reactances as obtained by closing the bend at its midsection by a magnetic and electric wall, respectively.

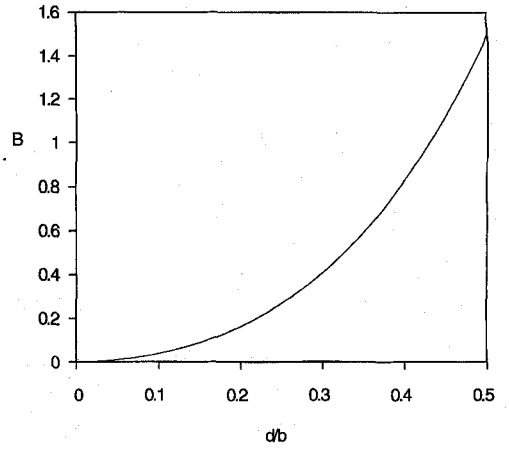

Fig. 7. Normalized admittance of a thin capacitive diaphragm.

This relationship is shown in Fig. 6 for the geometry under consideration, i.e., for a 90° bend in WR75 of radius $R = r + b/2 = 6$ mm, for which $\chi = 0.27$. For other types of bends, i.e., for different radii or angles, a similar relationship is also seen to hold, apart for the different values assumed by χ.

Since a symmetric junction is matched when $X_e = -1/X_o$ and by observing that the insertion of a thin conducting sheet, of any shape, in the symmetry plane of the bend changes just the even reactance, X_e, we may adjust this even reactance by inserting a thin diaphragm in the middle of the bend.

In order to determine whether the nature of the matching element is to be inductive or capacitive, we have modeled the bend as an equivalent transmission line of electrical length Θ since

$$X_e = -\frac{1}{\tan\Theta}. \tag{32}$$

After replacing the open circuit with a small admittance jB_L, the even input reactance in the matched situation, X_{eM}, becomes approximately

$$X_{eM} = -\frac{1 - B_L \tan\Theta}{B_L + \tan\Theta} \approx -\frac{1}{\tan\Theta} + B_L \frac{1 + \tan^2\Theta}{\tan^2\Theta} = X_e + B_L \frac{1 + \tan^2\Theta}{\tan^2\Theta}. \tag{33}$$

Therefore, since X_{eM} must be larger than X_e in order to match the bend, it follows that B_L has to be positive and consequently the diaphragm is capacitive.

The last formula provides also a tool for calculating B_L. In fact, by imposing that

$$X_{eM} = -1/X_o$$

we obtain

$$B_L = \frac{\chi}{1 + (1/X_o + \chi)^2}. \tag{34}$$

As already noted, in our case, $\chi \approx 0.27$ therefore $B_L \approx 0.137$ at midband. A first estimate of the height of the matching septum, can be obtained by [5, formula 2.c, p. 219], here

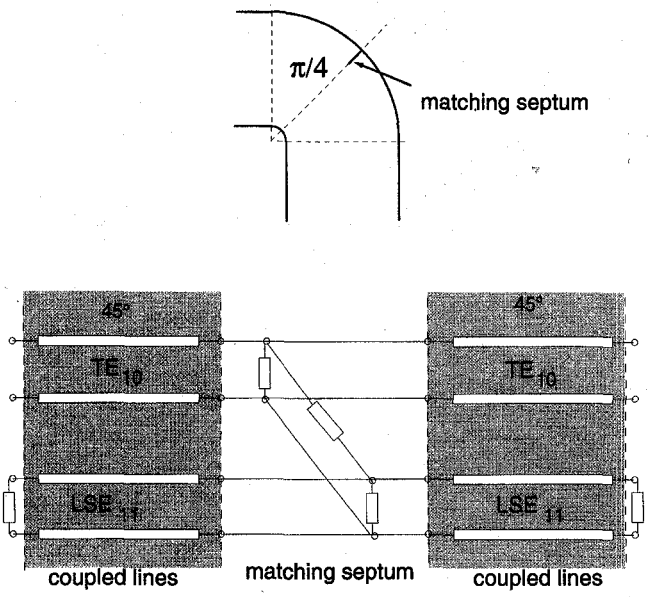

Fig. 8. A 90° matched bend and its multimodal equivalent circuit.

reported in Fig. 7, providing a values of normalized height $d/b \approx 0.185$, corresponding to 1.75 mm for WR75 waveguide.

Unfortunately, the circuit for a capacitive diaphragm provided by Marcuvitz, can not be used in conjunction with the multimode bend model, since the former considers as accessible just the propagating mode. In order to take full advantage of coupled mode analysis it is convenient to employ the equivalent circuit given in [15] which, as shown in Fig. 8, considers two accessible modes. Accordingly, the equivalent network of the 90° matched bend, upper figure in Fig. 8, is as represented by the equivalent circuit in the lower figure. This network can be easily analyzed by means of the coupled modes approach and the diaphragm height can be adjusted in order to improve the result provided by the Marcuvitz equivalent circuit. By doing so, the FBM 90° bend shown in Fig. 9 is obtained. From the latter figure it is apparent that low return loss (less than 30 dB) is achieved on the whole band of WR75 waveguide. For angles larger than 120° this matching procedure cannot be applied, since the relationship between

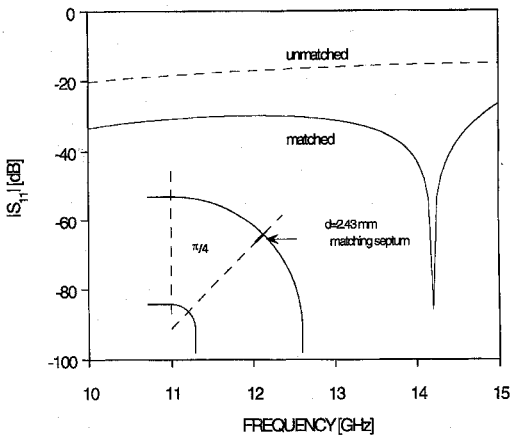

Fig. 9. Reflection coefficient of a matched E-plane 90° bend of radius $R = r + b/2 = 6$ mm in WR75.

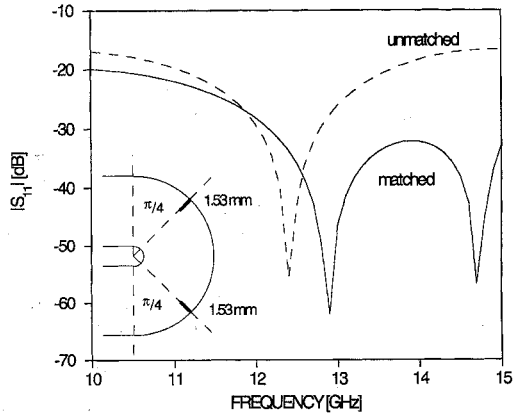

Fig. 10. Reflection coefficient of a matched E-plane 180° bend of radius $R = r + b/2 = 6$ mm in WR75.

the even and odd reactances of the bend, given by (31) does not hold. Good results can, however, be obtained by repeating the procedure on fractions of the total bend angle. For istance, in order to match a 180° bend, it is expedient to divide the bend into two bends of 90° and place a matching septum in the midplane of each. An example of the latter arrangement and relative return losses over the whole band is provided in Fig. 10.

Finally, it is worth mentioning that we have also checked the matching technique in the actual case of finite-thickness septa, simulating by a FDTD code an abrupt E-plane corner, matched by a finite thickness septum, obtaining, even in that more critical case, results comparable with those presented here.

VII. Conclusion

Full-band matched (FBM) waveguide bends with small radii of curvature have been realized by placing matching elements (ME) inside the curve. The design of FBM E-plane bends has been accomplished by using capacitive diaphragm(s) inside the curve as ME. A multimodal analysis of this configuration has been performed by using the local mode theory and the multimodal equivalent circuit of the diaphragm. This approach, while being extremely simple to implement, features numerical efficiency.

Acknowledgment

The authors would like to thank L. Accatino and R. Ravanelli for helpful discussions.

References

[1] H. H. Meinel, "Millimeter-wave technology advances since 1985 and future trends," *IEEE Trans. Microwave Theory Tech.*, vol. 39, pp. 759–767, May 1991.
[2] F. Alessandri, M. Mongiardo, and R. Sorrentino, "Computer-aided design of beam forming networks for modern satellite antennas," *IEEE Trans. Microwave Theory Tech.*, vol. MTT-40, no. 6, June 1992.
[3] F. Alessandri, M. Mongiardo, and R. Ravanelli, "A compact wide-band variable phase shifter for reconfigurable satellite beam forming networks," in *Proc. 23rd European Microwave Conf.*, 1993, pp. 556–557.
[4] F. C. de Ronde, "Full-band matching of waveguide discontinuities," in *MTT-S Int. Microwave Symp.*, Palo Alto, CA, 1966.
[5] N. Marcuvitz, *Waveguide Handbook*. New York: McGraw-Hill, 1951.
[6] M. Mongiardo and R. Sorrentino, "Efficient and versatile analysis of microwave structures by combined mode matching and finite difference methods," *IEEE Microwave and Guided Wave Lett.*, Aug. 1993.
[7] J. M. Reiter and F. Arndt, "A full-wave boundary contour mode-matching method (BCMM) for the rigorous CAD of single and cascaded optimized H-plane and E-plane bends," in *Proc. IEEE MTT-S Dig.*, 1994, pp. 1021–1024.
[8] Ke Li Wu, G. Y. Delisle, D. G. Fang, and M. Lecours, "Waveguide discontinuity analysis with a coupled finite-boundary element method," *IEEE Trans. Microwave Theory Tech.*, vol. 37, no. 6, pp. 993–998, June 1989.
[9] F. Alimenti, M. Mongiardo, and R. Sorrentino, "Design of mitered H-plane bends in rectangular waveguides by combined mode matching and finite differences," in *Proc. 24th Eu. M.C.*, Cannes, 1994.
[10] L. Accatino and G. Bertin, "Modal analysis of curved waveguides," in *Proc. 20th Eur. Microwave Conf.*, Budapest, Sept. 1990, pp. 1246–1250.
[11] A. Weisshaar, S. M. Goodnick, and V. K. Tripathi, "A rigorous method of moments solution for curved waveguide bends and its applications," in *Proc. IEEE MTT-S Dig.*, 1992, pp. 975–978.
[12] F. Alessandri, M. Mongiardo, and R. Sorrentino, "Rigorous mode matching analysis of mitered E-plane bends in rectangular waveguide," *IEEE Microwave and Guided Wave Lett.*, Dec. 1994.
[13] J. Uher, J. Bornemann, and U. Rosenberg, *Waveguide components for antenna feed systems: Theory and CAD*. Boston: Artech House, 1993, pp. 163–174.
[14] V. V. Shevchenko, *Continuous Transition in Open Waveguides*. Boulder, CO: Golem Press, 1971.
[15] T. Rozzi, "A new approach to the network modeling of capacitive irises and steps in waveguide," *IEEE Trans. Circuit Theory Applicat.*, vol. 3, pp. 339–354, 1975.

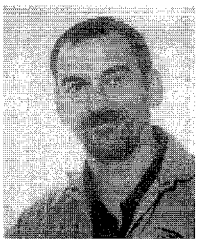

Mauro Mongiardo received the "Laurea" degree from the University of Rome (summa cum laude) and the Ph.D. degree from the University of Bath, U.K.

He is an Associate Professor at the University of Perugia in Italy. From 1983 he has been engaged on microwave radiometry, inverse problems, and in the experimental validation of a four-channel radiometer developed for temperature retrieval of biological bodies. He has been Visiting Scientist at the University of Victoria, B.C., Canada, working on time-domain analysis of MMIC. He is currently interested in the modeling and computer-aided design of microwave and millimeter wave guiding structure and antennas, and in the modeling of discontinuities in MMIC.

In 1988 he was recipient of a NATO-CNR research scholarship during which he was Visiting Researcher at the University of Bath (UK).

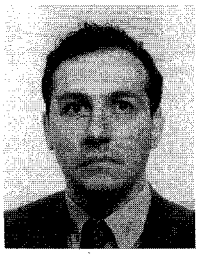

Antonio Morini received the degree in electronic engineering (summa cum laude) from the University of Ancona in 1987 and the Ph.D. degree in electromagnetism in 1992.

Since 1992 he has been with the Department of Electronics and Automatics at the University of Ancona as a Professor Assistant. His research is mainly devoted to the modeling and to the synthesis of passive millimetric wave devices, such as filters and multiplexers in rectangular waveguide, and antennas.

Tullio Rozzi (M'66-SM-74-F'90) received the "Dottore" degree in physics from the University of Pisa in 1965, and the Ph.D. degree in electronic engineering from Leeds University in 1968. In June 1987, he received the D.Sc. degree from the University of Bath, Bath, U.K.

From 1968 to 1978 he was a Research Scientist at the Philips Research Laboratories, Eindhoven, the Netherlands, having spent one year, 1975, at the Antenna Laboratory, University of Illinois, Urbana. In 1978 he was appointed to the Chair of Electrical Engineering at the University of Liverpool and was subsequently appointed to the Chair of Electronics and Head of the Electronics Group at the University of Bath, in 1981, where he also held the responsibility of Head of the School of Electrical Engineering on an alternate three year basis. Since 1988 Dr. Rozzi has been Professor of Antennas in the Department of Electronics and Control, University of Ancona, Italy, while remaining a visiting professor at Bath University.

Dr. Rozzi was awarded the Microwave Prize in 1975 by the IEEE Microwave Theory and Technique Society. He is also a Fellow of the IEE (U.K.) as well as IEE Council Representative for Italy.